Online Millimeter Wave Phased Array Calibration Based on Channel Estimation

Thomas Moon, Junfeng Gaun, Haitham Hassanieh

Electrical and Computer Engineering, University of Illinois at Urbana-Champaign, USA

Abstract—This paper proposes a new over-the-air (OTA) calibration method for millimeter wave phased arrays. Our method leverages the channel estimation process which is a fundamental part of any wireless communication system. By performing the channel estimation while changing the phase of an antenna element, the phase response of the element can be estimated. The relative phase of the phased array can also be obtained by collecting all the estimated phase responses with a shared reference state. Hence, the phase mismatches of the phased array can be resolved. Unlike prior work, our calibration method embraces all the array components such as power-divider, phase shifter, amplifier and antenna and thus, spans the full chain. By overriding channel estimation, our proposed technique does not require any additional circuits for calibration. Furthermore, the calibration can be performed online without the need to pause the communication. We tested our method on an eight element phased array at 24GHz which we designed and fabricated in PCB for verification. The measured beam pattens prove the viability of our proposed method.

Index Terms—Phased Array, Millimeter Wave, Calibration, Beamforming, Over-the-air measurement

I. INTRODUCTION

The surge of IoT and mobile devices has led to an explosive increase in demand for wireless bandwidth. This prompted the FCC to open multi-GHz of both license and unlicensed spectrum in the millimeter wave (mmWave) frequency bands above 24 GHz [1]. Millimeter wave is expected to deliver wireless link at fiber-like speeds of multi-Gbps and will play a central role in 5G cellular networks and future wireless LANs. However, mmWave signals attenuate quickly with distance. Hence, mmWave radios need to use directional antennas to focus the signal power and extend the range.

The key enabler for directionality in mmWave are phased arrays. The small wavelength of mmWave frequencies allow us to pack a very large number of antennas in a small area which creates highly directional narrow beams. Phased arrays allow us to electronically steer the direction of the beam in real-time in order to accommodate mobility and adapt to dynamic environments. A phased array works by changing the phase of the signal on each antenna element using a phase shifter. The phase shifter values are chosen in order to align the phase of the signals in a given direction θ to sum up constructively and beamform the signal towards θ.

However, due to the very small wavelength, mmWave phased arrays are extremely sensitive to small offsets in the design of the array and the output of the phase shifters. Specifically, process variation and RMS phase error of the phase shifters typically become significant at mmWave frequency
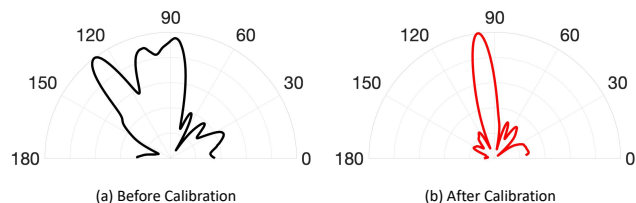

Fig. 1. Phased array beam pattern when directed towards $100°$ (a) before and (b) after calibration.

because the device feature size scales down [2]–[4]. Nanoscale transistors at mmWave frequency are more susceptible to long-term electrical stress. Even a single transistor aging can degrade circuit performance [5], [6]. Furthermore, temperature drifts also produce large degradation on the performance of phase shifting [7]. Without calibrating for these offsets and errors, the array can end up beamforming the signal in many directions which limits the gain of the array and the performance of the mmWave system while at the same time creating interference in other directions. Fig. 1 shows an example of the beam pattern of an 8 element phased array operating at 24 GHz before and after calibration. As can be seen, without calibration, the beam is not directional. It has more than one main lobe and a significant number of sidelobes.

Unfortunately, calibrating the phased array requires expensive equipment like vector network analyzers (VNAs) which can cost more than half a million dollars at mmWave frequencies [8] and cannot be used to calibrate mass production of mmWave phased arrays or recalibrate the arrays after being used. To reduce calibration cost and reliance on external test equipment, built-in self test (BIST) has been proposed as an alternative solution for phased array testing [9]–[13]. In [9], [10], [14], on-chip BIST circuitry is demonstrated: it is able to characterize and calibrate the amplitude and phase of each channel of the phased array. The BIST technique can generally achieve accurate measurements on the target system due to its proximity. To further reduce the test time on large scale phased arrays, parallel and tuning algorithms are presented in [12], [13]. The approach in [12] applies code-modulation to each element in the array to allow parallel measurements using BIST architecture on the distribution network. Concurrent testing on all mixed/RF components in MIMO is demonstrated using multiple test tones generated by BIST circuit [13].

The BIST approach, however, requires a special circuitry and its overhead becomes larger as the device size scales

down at mmWave frequency. The BIST circuitry generally forms a wire connection to the system under test which results in antenna mismatch that is not presented in the calibration process. The compatibility across package is another restriction to be considered in implementing BIST circuits. To address these issues, several researchers propose over-the-air (OTA) calibration of the phase and gain of phased array [15]–[19]. Some of these methods use amplitude-only measurement to estimate phase of each array element [16]–[18], while others use the mutual coupling of the array [15] or the scattering parameters of the probe antenna and the phased array to compute the excitations of the antenna elements [19]. Unfortunately, all these methods require a separate calibration process prior to using the phased array for communication and hence, cannot correct for errors that are triggered by transistor aging, electrical stress or temperature changes.

This paper presents a new online phased array calibration technique that enables calibrating the phased array during the communication process. This allows us to continuously calibrate the phased array without the need for expensive equipment, specialized circuitry or a separate calibration processes that can only be done prior to using the phased array for communication. The key idea is to leverage the wireless channel estimation protocol that is an inherent part of any wireless communication system. By changing the phase shifter values and monitoring how the phase and magnitude of the wireless channel changes in response, we can calibrate the phased array to maximize the received power and minimize the beam's sidelobes. Specifically, by performing the channel estimation while changing the phase of an antenna element, the phase response of the element can be estimated. The relative phase of the phased array can then be obtained by collecting all the estimated phase responses with a shared reference state which allows us to resolve the phase mismatches of the phased array. Our calibration method embraces all the array components such as power-divider, phase shifter, amplifier and antenna. Thus, the proposed method spans the full chain unlike prior work which is limited to a few selected components.

Since calibration takes place during the communication process, no additional measurements are required and in-field calibration is possible to adapt to system conditions such as temperature. We have implemented and tested our technique on a 24 GHz phased array with 8 antenna elements which we had designed and fabricated in PCB for verifications. Our results show that we can reduce the sidelobe leakage for the array by up to 7.3dB and our measured beam patterns prove the viability of our method.

II. PRIMARY

A. Phased Array

A phased array system is composed of an array of antenna elements that is spaced with a distance d as shown in Fig. 2. Each antenna element is connected to a phase shifter that is capable of changing the phase of the input signal. If a signal is arrived at a certain angle, θ, the distance traveled by the signal at the antenna element will be different by $d \cos \theta$ with
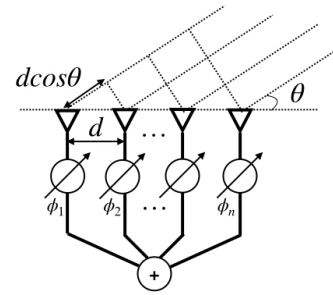

Fig. 2. **Phased Array System.** Phased array system can steer a beam at a direction θ by shifting the phase of signals.

its neighbor element. Mathematically, the power P of signals arriving along the direction θ can be written as:

$$P(\theta) = \sum_{n=1}^{N_p} e^{j2\pi \frac{nd\cos\theta + \phi_n}{\lambda}} \tag{1}$$

where ϕ_n is the phase change by the n-th phase shifter and λ is the wavelength of the signal. By setting the phase shift ϕ_n equal to $-nd\cos\theta$, the power is maximized at the direction θ, and thereby the beam is steered to the desired direction.

B. Channel Estimation

In wireless communication, the received signal is corrupted by the channel response such as attenuation, phase shift, and noise. Therefore, estimating and correcting the channel is one of the key processes to recover the symbols at the receiver. Even our proposed method works with any wireless communication schemes, we use Orthogonal Frequency-Division Multiplexing (OFDM) not only because it is one of prominent communication scheme in WiFi and LTE but also because its channel estimation is simple and efficient to be implemented.

Wireless signals transmitted over the air suffer inter-symbol interference (ISI) due to multipath channel effect and frequency-selective fading. In conventional single-carrier system, complicated equalization techniques are adopted to solve the issues. To combat these problem, multi-carrier modulation scheme is developed. OFDM divides a spectrum band into many small and partially overlapping subcarriers, and modulates the symbols on the subcarriers. The subcarriers are chosen to be orthogonal so that the inter-carrier interference sums up zero. The OFDM output signal at the transmitter is given by

$$x(t) = \sum_{k=0}^{N-1} X(f_k)e^{j\frac{2\pi f_k t}{N}} \tag{2}$$

where f_k is the k-th subcarrier frequency. The above equation is an N-point inverse discrete Fourier transform (IDFT), which can be implemented in Fast Fourier transform requiring only $O(N \log N)$ computation. Once the transmitter performs the IFFT to convert the symbols in the frequency domain to N time domain samples, the receiver converts the signal back to the frequency domain using the FFT, where each subcarrier is demodulated independently.

Let $X_{i,k}$ is the transmitted OFDM symbol at the time index i and the frequency index k. The received OFDM symbol $R_{i,k}$ can be written as

$$R_{i,k} = H_k X_{i,k} + w \qquad (3)$$

where H_k is the frequency response of the channel at k-th frequency index and w is the additive Gaussian white noise (AWGN). If a pilot OFDM symbol at $i = -1$ is sent before the data OFDM symbols ($i = 0, 1, 2, ...$), H_k can be estimated by the Least Squares (LS) method as:

$$\hat{H}_k = \frac{R_{-1,k}}{X_{-1,k}} \qquad (4)$$

Therefore, the channel estimation in OFDM can be performed in much simpler way than the conventional communication scheme.

III. PROPOSED METHOD

A. Channel Model for Phased Array

Consider the channel including N_p number of phase shifters. The received OFDM symbols can be written as

$$R_{i,k} = H_k X_{i,k} \qquad (5)$$

$$= \left(a_0 e^{j\phi_0} + \sum_{n=1}^{N_p} a_n e^{j\phi_n}\right) X_{i,k} \qquad (6)$$

where a_n and ϕ_n are the magnitude and phase response of n-th antenna element, respectively. The leakage of the phased array is represented by $a_0 e^{j\phi_0}$. To see how a phase shifter contributes to the channel, the channel constellation measured at the receiver is shown in Fig. 3 (a). As described in Equation 6, the total channel is the sum of the complex numbers whose values are determined by the response of the phase shifters and the leakage. If one of the array element changes its phase from 0 to 2π, the channel constellation will rotate a full circle. Therefore, the trajectory of the channel constellation can indicate the response of an element.

As described in the previous section, the channel can be estimated by sending a pilot symbol at the time index $i = -1$. The frequency response of the channel from H_0 to H_{N-1} at a given time can be obtained simultaneously. Therefore, the measurement on wideband frequency response comes with free by adopting OFDM scheme.

B. Formalizing the Problem

In practice, the magnitude and phase response of antenna element has more complicated form than described in Equation 6. If we look closely into one element, the response of one element can be written as a function of the control state, s:

$$f_n(s) = a_n(s) e^{j\phi_n(s) + \varphi_n} \qquad (7)$$

where φ_n is a constant phase mismatch.

There are two problems. First, the functions $a_n(s)$ and $\phi_n(s)$ are not identical over different element n. Therefore, the magnitude and phase are unknown at a given state. Second, even they are assumed to be identical over different element,
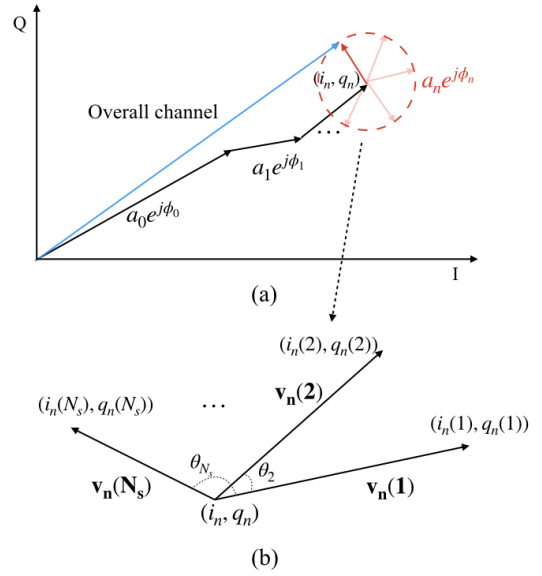

Fig. 3. **Channel Estimation Constellation.** (a) Each phase shifter contributes to the overall channel response. (b) The response of phase shifter is determined by a given model. Changing the control state of the phase shifter will move the channel response.

the phase mismatch term, φ_n, is unknown in general. The phase mismatch is often dependent on the other components such as power divider and antenna which are independent with the state.

In this paper, we assume the response of the phase shifters are not randomly different but share a similar characteristic. In section III-C, the shared model will assist to enhance the estimation. Consequently, the phase mismatch can be resolved in section III-D.

C. Model-assisted Phase Estimation

We assume the phase shifters shares a common magnitude and phase response that is known in priori. However, due to manufacturing variation and mismatch, their output measurements are not identical. For example, two phase shifters can share a common response but can create two different channel constellations. The actual constellation of the phase shifters can be different due to 1) different magnitude and phase response to control state, 2) relative phase offset, and 3) noise. In practice, the magnitude response is not flat over the phase shifts. Thus, the constellation does not necessarily form a circle while the phase is shifting from 0 to 2π, which makes the estimation difficult.

Suppose (i_n, q_n) is the unknown center of the trajectory on the constellation of the n-th element and $(i_n(1), q_n(1)), (i_n(2), q_n(2)), ..., (i_n(N_s), q_n(N_s))$ are the measurements at N_s discrete phase states. The objective is to find the best estimate of the center given the measurements and the model response. Consider the vectors $\mathbf{v_n}(1) = [i_n(1), q_n(1)]^T - [i_n, q_n]^T$ and $\mathbf{v_n}(2) = [i_n(2), q_n(2)]^T - [i_n, q_n]^T$ as shown in Fig. 3 (b).

$\mathbf{v_n(2)}$ can be obtained by rotating θ_2 and scaling c_2 on $\mathbf{v_n(1)}$. It can be described as

$$\mathbf{S}(c_2)\mathbf{R}(\theta_2)\mathbf{v_n(1)} = \mathbf{v_n(2)} \tag{8}$$

$$\mathbf{S}(c_2)\mathbf{R}(\theta_2)\begin{bmatrix} i_n(1) - i_n \\ q_n(1) - q_n \end{bmatrix} = \begin{bmatrix} i_n(2) - i_n \\ q_n(2) - q_n \end{bmatrix} \tag{9}$$

$$\begin{bmatrix} i_n(2) \\ q_n(2) \end{bmatrix} - \mathbf{S}(c_2)\mathbf{R}(\theta_2)\begin{bmatrix} i_n(1) \\ q_n(1) \end{bmatrix} = \left(\mathbf{I} - \mathbf{S}(c_2)\mathbf{R}(\theta_2)\right)\begin{bmatrix} i_n \\ q_n \end{bmatrix} \tag{10}$$

By defining

$$\mathbf{y_m} = \begin{bmatrix} i_n(m) \\ q_n(m) \end{bmatrix} - \mathbf{S}(c_m)\mathbf{R}(\theta_m)\begin{bmatrix} i_n(1) \\ q_N(1) \end{bmatrix} \tag{11}$$

$$\mathbf{a_m} = \mathbf{I} - \mathbf{S}(c_m)\mathbf{R}(\theta_m) \tag{12}$$

, Equation 10 can be written as:

$$\mathbf{y_2} = \mathbf{a_2}\mathbf{x} \tag{13}$$

where $\mathbf{x_n}$ is the unknown center $\begin{bmatrix} i_n \\ q_n \end{bmatrix}$, $\mathbf{S}(c)$ is the scaling matrix $\begin{bmatrix} c & 0 \\ 0 & c \end{bmatrix}$ and $\mathbf{R}(\theta)$ is the rotation matrix $\begin{bmatrix} \cos\theta & -\sin\theta \\ \sin\theta & \cos\theta \end{bmatrix}$.

Note that matrix S and R are determined by the model. 2-by-2 system matrix in Equation 13 can be expanded to $2(N_s - 1)$-by-2 system by observing all N_s constellation points as follows:

$$\begin{bmatrix} \mathbf{y_2} \\ \mathbf{y_3} \\ \vdots \\ \mathbf{y_{N_s}} \end{bmatrix} = \begin{bmatrix} \mathbf{a_2} \\ \mathbf{a_3} \\ \vdots \\ \mathbf{a_{N_s}} \end{bmatrix} \mathbf{x_n} \tag{14}$$

$$\mathbf{Y} = \mathbf{A}\mathbf{x_n} \tag{15}$$

The above system is linearly over-determined, $2(N_s - 1)$ observations for two unknowns. It is a linear regression problem that estimates the unknown model parameter, $\mathbf{x_n}$, from the data. Linear least square estimation minimized the sum of squared residuals:

$$\hat{\mathbf{x_n}} = (\mathbf{A^T A})^{-1}\mathbf{A^T Y} \tag{16}$$

where $\hat{\mathbf{x_n}} = \begin{bmatrix} \hat{i_n} \\ \hat{q_n} \end{bmatrix}$ is the least squared estimation for the center.

D. Phase Mismatch Calibration

Once we estimated the center of the n-th element, the magnitude and phase of state m can be calculated as:

$$a_n(m) = |\hat{\mathbf{v_n}}(\mathbf{m})| \tag{17}$$
$$\phi_n(m) = \angle \hat{\mathbf{v_n}}(\mathbf{m}) \tag{18}$$

where $\hat{\mathbf{v_n}}(m) = \begin{bmatrix} i_n(m) \\ q_n(m) \end{bmatrix} - \hat{\mathbf{x}}$.

The relative phase mismatch between the antenna elements can be calculated by comparing the phase at a reference state. For example, we set the first element as the reference element and the first state as the reference state. The relative phase between the reference element and the n-th element is equal to the difference of the phase at the reference states.

$$\Delta\phi_n = \phi_n(1) - \phi_1(1) \tag{19}$$

It is a reasonable assumption that the phase offset is independent with the control state and has a fixed constant value for each element because the sources of the mismatch are often passive components such as power divider and patch antenna.

E. Handling Synchronization Offsets

In order to achieve a correct channel estimation on wireless channel, the transmitter and receiver are required to be synchronized by estimating and canceling the carrier frequency offset (CFO) and sampling frequency offset (SFO). The estimation of the CFO/SFO will be affected while changing the phase of the antenna. This issue can be resolved by adding a single static antenna on each Tx and Rx to form a static channel. The CFO/SFO estimation on the static channel can be used to cancel the frequency offset between Tx/Rx, and thus the synchronization can be achieved during the phase changes.

IV. HARDWARE IMPLEMENTATION

We designed and built a mmWave phased array system to evaluate the proposed method. The hardware block diagram shown in Fig. 4 (a) is implemented by the commercial off-the-shelf components. NI USRP-2920 is used for an IF and baseband signal processing unit and transmites/receives OFDM baseband signals. We use HMC815 and HMC977 evaluation board for 24GHz I/Q up-converter and down-converter, respectively. The up/down-converts include an internal power amplifier/LNA, an IQ mixer, and a frequency doubler. We use LMX2594 PLL evaluation board to generate the LO signal at 11GHz for the IQ up/down-converters. A prototype phased array test board was fabricated on printed circuit board (PCB) on Rodgers substrate as shown in Fig. 4 (b). The power splitter and the patch antenna were simulated and designed by Advanced Design System. The phased array board includes 8 antenna elements spaced by $\lambda/2$. The RF input signal is splitted by the transmission line and fed into 24GHz analog phase shifters (HMC-933). The control voltage for the phased shifter is generated by a 8-bit DAC (AD7228A). The DAC is controlled by Arduino Duo micro-controller which is synchronized with USRP through the PC. For calibration and measurement, the phased array is used for the transmitter antenna. We use a K-band horn antenna from SAGE for the receiver antenna. The horn antenna has 22dBi gain and 12 degree 3dB beamwidth.

V. EXPERIMENTAL RESULTS

The proposed calibration method is evaluated on 8-element 24GHz phased array. To calibrate the phased array on the transmitter, we use the horn antenna at the receiver side facing toward transmitter. The control voltage is swept from 0V to 10V while the transmitter and the receiver are communicating OFDM packets. Fig. 5 shows the measured channel constellation at two different elements. We import the magnitude
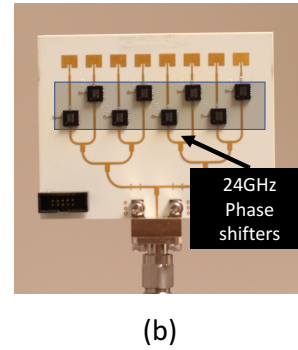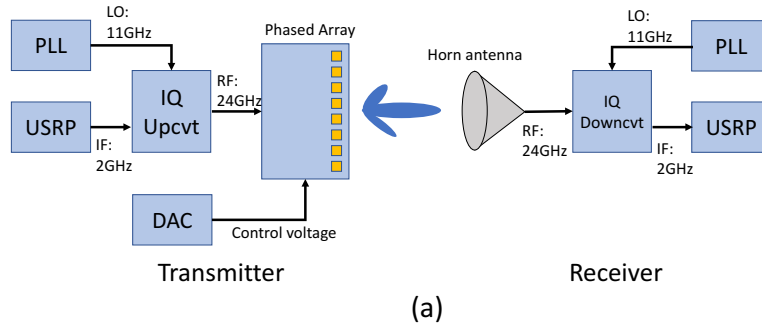
Fig. 4. **Hardware Block Diagram and Phased Array.** (a) Block diagram of the mmWave transmitter and receiver system we built. (b) The 8-element phased array. Each 24GHz phase shifter is connected to a patch antenna. The control voltage is provided by an external DAC through the connector.
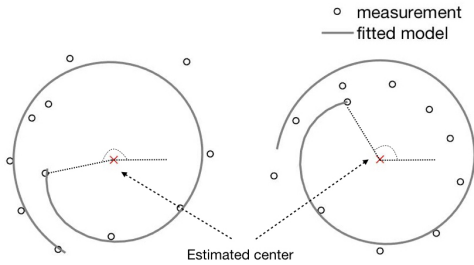

Fig. 5. **Measured Channel Estimation and Model.** The figure shows the channel estimation from two phase shifters with the fitted model. The relative phase can be evaluated by comparing the reference state.
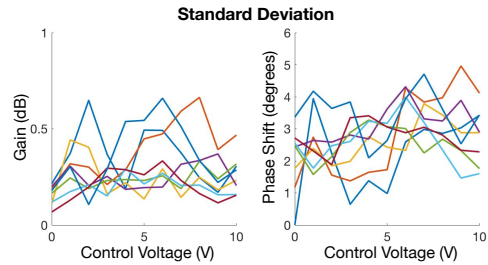

Fig. 7. **Stability of Calibration.** Standard deviation of calibration result. The figure shows that the calibration is stable within 1dB gain deviation and 5 degree phase deviation.
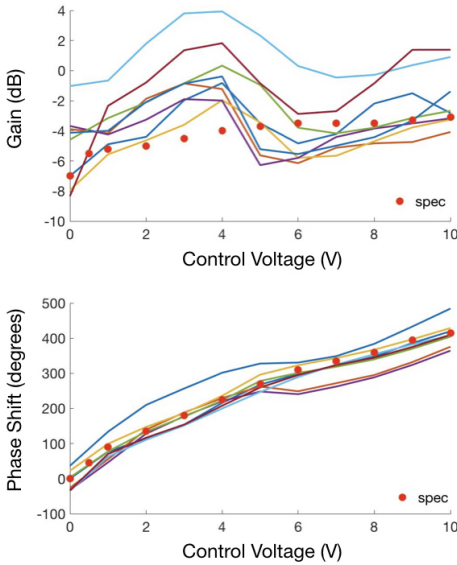

Fig. 6. **Estimated Gain and Phase.** The figure shows the estimated gain and phase of the 8 phase shifters over the control voltage. The red dots shows the specification of the phase shifter.
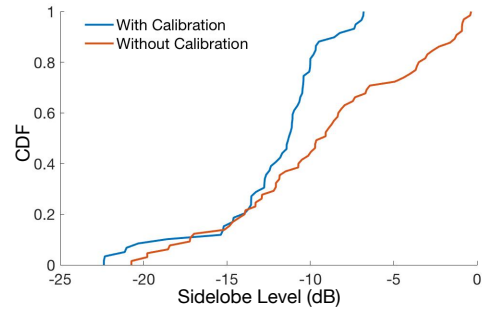

Fig. 8. **Performance of Calibration.** CDF of sidelobe level relative to the main beam with and without calibration. The figure shows that calibration significantly reduces the radiation outside of the main beam.

the beam pattern without a proper calibration. In Fig. 7, the standard deviation of the gain and phase calibration result is shown. The result shows the calibration is stable enough that the standard deviation of the gain and phase are less than 1dB and 5 degree, respectively.

To evaluate the beam pattern with calibration, the phased array is mounted on a pole equipped with a precise step motor. We setup the phase shifters of the array to steer at a specific angle, then we rotate the phased array antenna from 0-180 degrees while the horn antenna is receiving the transmitted signal. We measure the received power at each angle which gives us the radiation pattern. In Fig. 9, we set the phased array to steer the beam at 9 different angles (50-130 degree, 10 degree step) and compare the beam patterns with and without calibration. For the sake of clarification, the peak magnitude is

and phase specification of the phase shifters (HMC-933) and estimate the center for the trajectory. We run the calibration 10 times for each 8 element. The gain and phase estimated for the 8 elements by the channel estimation is plotted in Fig. 6. The red circles represents the specification of the phase shifter. The figure shows that a few phase shifters have a huge phase offset more than 100 degree. This phase mismatch will degrade
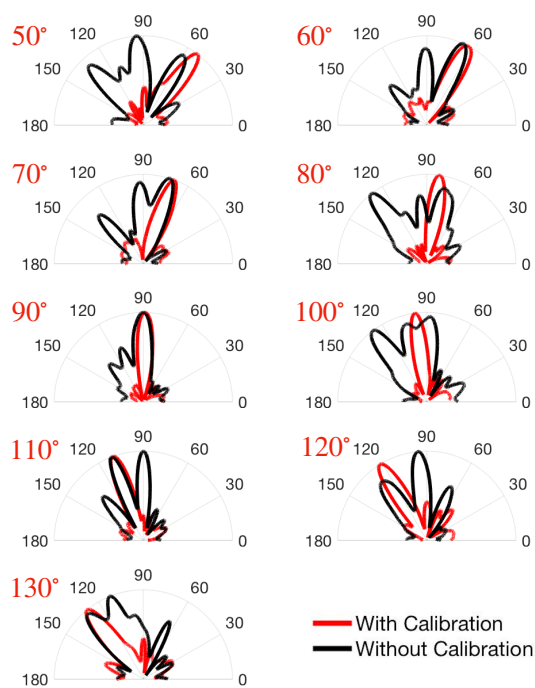
Fig. 9. **Beam Patterns.** The measured beam patterns steered at 9 different angles are shown. The beam patterns before (black) and after (red) calibration are compared. The peak magnitude is normalized for better visualization.

normalized in both cases. In general, the peak power without the calibration is smaller than with the calibration because the signal power is not focused at one direction. The beam pattern with calibration shows that the main lobe is narrower and the side lobe levels are lower than without calibration. For each measured beam pattern, we calculate the side lobe level (SLL) which is the side lobe power relative the main lobe. Higher SLL means that the antenna leaks more power outside the main lobe. Fig. 8 compares the CDF of SLL with and without calibration. The 90th percentile of SLL is -1.3dB without calibration, while it reduces to -8.6dB with calibration. The result implies that calibration reduces side lobe power and improves the directionality of the phased array.

We observed that the beam patterns with calibration still have higher side lobes than the theoretical value. The main reason for this is because of the magnitude mismatch between the elements. We do not calibrate the magnitude mismatch in this work because our hardware does not support the control over the magnitude for each element. This problem will be further studied in the future work.

VI. Conclusion

In this paper, we present a new online OTA calibration method for mmWave phased array. Due to the small wavelength, mmWave phased array is very sensitive to small offsets, which makes calibration difficult. Our method exploits channel estimation in wireless communication in order to measure the magnitude and phase response of the phased array system. Therefore, our calibration can be online not necessarily to pause the communication and does not need extra circuits.

We implemented an 8-element 24GHz phased array system to evaluate our calibration. The hardware measurement results prove that our calibration is capable of compensating the phase mismatches and improves the beam pattern by reducing SLL.

References

[1] A. Pai, "Keeping up a fast pace on spectrum," https://www.fcc.gov/news-events/blog/2018/10/01/keeping-fast-pace-spectrum, FCC, 2018.

[2] A. Sethi, J. P. Aikio, R. A. Shaheen, R. Akbar, T. Rahkonen, and A. Parssinen, "A 10-bit active rf phase shifter for 5g wireless systems," in *Nordic Circuits and Systems Conference (NORCAS): NORCHIP and International Symposium of System-on-Chip (SoC), 2017 IEEE*. IEEE, 2017, pp. 1–4.

[3] D. Chen, X. Zhang, L. Zhang, Z. Chen, S. Sun, Y. Liu, C. Zhao, H. Liu, Y. Wu, and K. Kang, "A ku-band 8-element phased-array transmitter with built-in-self-test capability," in *2018 IEEE/MTT-S International Microwave Symposium-IMS*. IEEE, 2018, pp. 610–612.

[4] J. Y.-C. Liu, Z. Xu, Q. J. Gu, and M.-C. F. Chang, "Self-healing techniques for robust mm-wave power amplification," in *RF and Mm-Wave Power Generation in Silicon*. Elsevier, 2016, pp. 381–408.

[5] J. Yuan, Y. Xu, S. Yen, Y. Bi, and G. Hwang, "Hot carrier injection stress effect on a 65 nm lna at 70 ghz," *IEEE Transactions on Device and Materials Reliability*, vol. 14, no. 3, pp. 931–934, 2014.

[6] L. Chang, Y.-K. Choi, D. Ha, P. Ranade, S. Xiong, J. Bokor, C. Hu, and T.-J. King, "Extremely scaled silicon nano-cmos devices," *Proceedings of the IEEE*, vol. 91, no. 11, pp. 1860–1873, 2003.

[7] C.-Y. Kim, D.-W. Kang, and G. M. Rebeiz, "A 44–46-ghz 16-element sige bicmos high-linearity transmit/receive phased array," *IEEE Transactions on Microwave Theory and Techniques*, vol. 60, no. 3, pp. 730–742, 2012.

[8] Keysight, "Pna network analyzers, 900 hz to 120 ghz," https://www.keysight.com/en/pcx-x205186/pna-network-analyzers-300-khz-to-11-thz, 2018.

[9] S. Y. Kim, O. Inac, C.-Y. Kim, and G. M. Rebeiz, "A 76–84 ghz 16-element phased array receiver with a chip-level built-in-self-test system," in *Radio Frequency Integrated Circuits Symposium (RFIC), 2012 IEEE*. IEEE, 2012, pp. 127–130.

[10] O. Inac, F. Golcuk, T. Kanar, and G. M. Rebeiz, "A 90–100-ghz phased-array transmit/receive silicon rfic module with built-in self-test," *IEEE Transactions on Microwave Theory and Techniques*, vol. 61, no. 10, pp. 3774–3782, 2013.

[11] M. Margalef-Rovira, M. Barragan, E. Sharma, P. Ferrari, E. Pistono, and S. Bourdel, "An oscillation-based test technique for on-chip testing of mm-wave phase shifters," in *VLSI Test Symposium (VTS), 2018 IEEE 36th*. IEEE, 2018, pp. 1–6.

[12] K. Greene, V. Chauhan, and B. Floyd, "Built-in test of phased arrays using code-modulated interferometry," *IEEE Transactions on Microwave Theory and Techniques*, vol. 66, no. 5, pp. 2463–2479, 2018.

[13] S. Deyati, B. J. Muldrey, B. Jung, and A. Chatterjee, "Concurrent built in test and tuning of beamforming mimo systems using learning assisted performance optimization," in *Test Conference (ITC), 2017 IEEE International*. IEEE, 2017, pp. 1–10.

[14] J. W. Jeong, J. Kitchen, and S. Ozev, "A self-compensating built-in self-test solution for rf phased array mismatch," in *Test Conference (ITC), 2015 IEEE International*. IEEE, 2015, pp. 1–9.

[15] H. M. Aumann, A. J. Fenn, and F. G. Willwerth, "Phased array antenna calibration and pattern prediction using mutual coupling measurements," *IEEE Transactions on Antennas and Propagation*, vol. 37, no. 7, pp. 844–850, 1989.

[16] S. Mano and T. Katagi, "A method for measuring amplitude and phase of each radiating element of a phased array antenna," *Electronics and Communications in Japan (Part I: Communications)*, vol. 65, no. 5, pp. 58–64, 1982.

[17] T. Takahashi, H. Miyashita, Y. Konishi, and S. Makino, "Theoretical study on measurement accuracy of rotating element electric field vector (rev) method," *Electronics and Communications in Japan (Part I: Communications)*, vol. 89, no. 1, pp. 22–33, 2006.

[18] R. Long, J. Ouyang, F. Yang, W. Han, and L. Zhou, "Fast amplitude-only measurement method for phased array calibration," *IEEE Transactions on Antennas and Propagation*, vol. 65, no. 4, pp. 1815–1822, 2017.

[19] ——, "Multi-element phased array calibration method by solving linear equations," *IEEE Transactions on Antennas and Propagation*, vol. 65, no. 6, pp. 2931–2939, 2017.